Occurrence of Birefringent Retinal Inclusions in Cynomolgus Monkeys After High Doses of Canthaxanthin

Regina Goralczyk, Susanne Buser,† Jochen Bausch,* Walter Bee,‡ Ulrich Zühlke,‡ and Felix M. Barker§*

Purpose. To reproduce and investigate in a primate animal model the phenomenon of the red carotenoid canthaxanthin (β,β-carotene-4'4'-dione) to induce crystal-like retinal deposits as they have been observed in the ocular fundus of humans after high canthaxanthin intake (i.e., more than 30 mg/day).

Methods. Groups of four cynomolgus monkeys (*Macaca fascicularis*) per gender and dose were administered 5.4, 16.2, or 48.6 mg canthaxanthin/kg body weight daily by oral gavage for 2.5 years. Eight control animals received placebo. In vivo ophthalmoscopy was performed at intervals of 3 months along with electroretinography after 12 and 24 months and retinal biomicroscopy just before the monkeys were killed. Retinal wholemounts or frozen sections were investigated postmortem by polarization, bright field, and differential interference contrast microscopy. Retinal and preterminal plasma canthaxanthin concentrations were determined by high-performance liquid chromatography (HPLC).

Results. By ophthalmoscopy and retinal biomicroscopy in vivo, no crystals or other light-reflecting particles were observed in the central paramacular retina. However, postmortem polarization microscopy of all 24 canthaxanthin-treated animals showed a circular zone in the peripheral retina containing birefringent, polymorphous red, orange, or white inclusions. The density of these inclusions was diminished within 1 to 8 mm posterior to the ora serrata. These inclusions were located mainly in the inner retinal layers, that is, the nerve fiber layer and ganglion cell layer, inner plexiform layer, and inner nuclear layer. Twelve of the 24 canthaxanthin-treated animals showed yellow, golden birefringent inclusions in the macula. Retinas of placebo-treated monkeys were free of birefringent, crystal-like inclusions. The HPLC confirmed the presence of all-trans canthaxanthin, and 4-OH-echinenone and isozeaxanthin as well, in the retinas of all canthaxanthin-treated animals. Neither electroretinography nor histopathology indicated any adverse effects of the canthaxanthin-induced retinal inclusions seen in this study.

Conclusions. A high intake of canthaxanthin for 2.5 years led to the deposition of crystal-like birefringent inclusions in the inner layers of the peripheral retina and, to some extent, the central retina of cynomolgus monkeys. The presence of these deposits did not interfere with morphology nor with retinal function. Invest Ophthalmol Vis Sci. 1997;38:741–752.

The carotenoid canthaxanthin (β,β-carotene-4'4'-dione) is synthesized in nature by the mushroom *Cantharellus cinnabarinus*. It also occurs in a variety of other plants and animals (e.g., in algae, Crustacea, birds, or fish). Because of its intense red color, canthaxanthin is used for both direct or indirect food coloring. In humans, canthaxanthin is deposited in the skin where it has been shown to be a free radical and singlet oxygen quencher.[1] Based on these properties, a combination of canthaxanthin and β-carotene (Phenoro, F. Hoffmann-La Roche, Basel, Switzerland) has been used since the beginning of the 1970s as a dermal photoprotector in diseases such as polymorphous photodermatoses and erythropoietic protoporphyria. Furthermore, the skin coloring effect led to the development of so-called "tanning pills" (Orobronze, Applipharm, Marseille, France) to imitate sun tan. Since 1982,[2] reports have been published describing glittering crystalline inclusions in the retina of humans after high

*From *Vitamins & Fine Chemicals, Department of Exploratory Research, and †Pharma Division, Preclinical Research, Department of Toxicology, F. Hoffmann–La Roche AG, CH-4070 Basel, Switzerland; ‡Corning Hazleton GmbH, D-48163 Münster, Germany; and §Light and Laser Institute, Pennsylvania College of Optometry, Philadelphia, Pennsylvania.*
Submitted for publication August 14, 1996; revised October 23, 1996; accepted October 25, 1996.
Proprietary interest category: E(RG, SB, JB); C2(WB, UZ); C38(FB).
Reprint requests: Regina Goralczyk, Vitamins & Fine Chemicals, Department of Exploratory Research, Building 93/822, F. Hoffmann–La Roche AG, Grenzacher str. 124 CH-4070 Basel, Switzerland.

dosage or long-term intakes or both of this carotenoid either for cosmetic skin coloring or medical purposes (reviewed by Arden and Barker[3]). In these reports, golden yellow glistening crystals were observed by routine ophthalmoscopy, occurring typically in a perimacular ring configuration. In an anecdotal postmortem investigation of a human,[4] crystal-like inclusions were found in a perimacular ring but also were found in a peripheral zone of the retina. In this report, high-performance liquid chromatography (HPLC) analysis and microphotometry showed that canthaxanthin was present in the sample tissue.

The deposition of crystal-like formations in the human retina typically has been associated with high dosages or prolonged canthaxanthin intakes or both, with crystals not likely to form at dosage levels <30 mg/day.[5] Various ocular diseases have been shown to increase the degree of crystalline retinopathy.[6] People having these retinal inclusions typically are without associated visual symptoms or clinically measurable dysfunctions, including clinically normal electrophysiological responses.[3]

Several animal studies were performed to investigate these phenomena and to clarify the question concerning the safety of canthaxanthin in medical and food applications. However, all attempts to reproduce retinal canthaxanthin crystals in species such as cats,[7] rabbits,[8] ferrets,[9] dogs, or rodents (unpublished data) have failed. Only recently, canthaxanthin crystal formation has been shown in vitro in chick embryonic retina cells if they were cultured in the presence of canthaxanthin bound to chicken high-density lipoproteins (Bruinink et al, in preparation). In addition, there were some earlier indications that traces of crystals form histologically in the retina of canthaxanthin-treated monkeys.[10] This primate species and humans have a similar carotenoid metabolism, and both deposit the carotenoids zeaxanthin and lutein as yellow macular pigments in the retina,[11–13] thus raising the possibility of using the monkey as a model for experimental canthaxanthin studies.

The question whether and how canthaxanthin forms crystals in the retina remains a topic of interest, especially because of the increasing demand for specific carotenoids, including canthaxanthin, as free radical and singlet oxygen quenchers and as antioxidants.[14] Thus carotenoids have the potential to act as preventive or therapeutic photoprotectors, particularly in the retina.[15] We performed a study with cynomolgus monkeys (*Macaca fascicularis*) to test whether these animals are a suitable model for canthaxanthin-induced retinal crystal deposition and to determine whether the crystals have an effect on retinal function.

MATERIALS AND METHODS

Chemicals

A commercial, cold water-soluble carotenoid beadlet formulation (Dry Canthaxanthin 10% WS, F. Hoffmann-La Roche, Basel, Switzerland), containing 10% canthaxanthin (β,β-carotene-4′4′-dione); all-rac-α-tocopherol and ascorbyl palmitate as stabilizer; vegetable oil; gelatine; sucrose; and corn starch as carrier, was used as test material. Canthaxanthin content by chemical analysis was 11.6%, with approximately 80% trans and 20% cis-isomers. The canthaxanthin-derived compounds 4-OH-echinenone and isozeaxanthin were not detectable in the beadlet formulation. Placebo powder contained all ingredients except the carotenoid. Pure, crystalline canthaxanthin was used as HPLC standard.

Animal Husbandry and Method of Carotenoid Application

The study was performed at Corning Hazleton GmbH, Münster, Germany, under Good Laboratory Practice conditions and according to the guidelines for animal trials in the EEC and the ARVO Statement for the Use of Animals in Ophthalmic and Vision Research. Cynomolgus monkeys were housed in individual cages and exposed to a constant artificial light cycle (12 hours light/12 hours dark). The basic diet (Ssniff p 10 pellets; Ssniff Spezialdiäten GmbH, 59494 Soest, Germany) was offered twice a day. In addition, fruits were given twice a week, a slice of bread once a week. Four male and four female cynomolgus monkeys were assigned for each dose group. The amount of canthaxanthin powder necessary to achieve the target doses of 5.4, 16.2, and 48.6 mg/kg/body weight per day was solubilized in 4 ml water (40°C) and administered by oral gavage once a day. The solutions were prepared freshly each day. Placebo was administered to the control animals in amounts equivalent to the canthaxanthin formulation required to achieve a target dose of 16.2 mg/kg body weight per day.

In Vivo Retinal Examination

The eyes of all animals were examined before the start of treatment and in intervals of approximately 3 months during the trial. Examinations were conducted with the animals under sedation (10 mg/kg ketamine hydrochloric acid, Ketavet, Parke-Davis, Freiburg, Germany) and with pupil dilation (Mydriaticum Roche, F. Hoffmann-La Roche, Grenzach, Germany). Examinations were performed using both direct and indirect ophthalmoscopy. A slit-lamp biomicroscope (Zeiss, Jena, Germany) also was used to examine the anterior segment and, before the animals were killed, to examine the central retina using a Goldmann 3-mirror lens and a Volk 90 D lens. Retinal photodocumentation was made for selected cases (Kowa RC-2, Düsseldorf, Germany).

Electroretinography

Visual function was tested by electroretinography (ERG) performed on all animals at 12 and 24 months.

For the ERGs, the animals were sedated (10 mg/kg ketamine hydrochloric acid, Ketavet, Parke-Davis, and 0.3 mg/kg diazepam, Valium, F. Hoffmann-La Roche) with their pupils dilated (Homatropine-HBr, Ursapharm, Saarbruckem, Germany) and their corneas anesthetized (Chibro-Kerakain, Chibret, Haar, Germany). A standardized ERG protocol[16] based on the International Society for Clinical Electrophysiology (ISCEV[17]) was used. It included seven scotopic responses with increasing flash intensity, oscillatory potentials, two 30-Hz flicker, and three red flash and one white flash photopic recording. Additionally, ERGs were recorded at low-flash intensity during 32 minutes of dark adaptation.

Light stimulation for the ERGs was produced with a Nicolet Compact Visual Ganzfeld dome (Nicolet Instrument GmbH, Offenbach, Germany) illuminated by a xenon stroboscopic flash. The ERGs were recorded using contact lens electrodes (Universo, Le Chaux de Fonds, Switzerland) and the Nicolet recording system.[16] The peak amplitude and latency of each response were evaluated. Data were subjected to analysis of variance and covariance with repeated measurements (GLM procedure; SAS Institute, Cary, NC). In performing the data analysis, the values obtained from the placebo and canthaxanthin-treated groups also were compared to data obtained from a collective of 23 untreated monkeys analyzed over 3 years at Corning Hazleton GmbH.

Necropsy

Animals were killed after approximately 31 months. The monkeys were euthanized by an intravenous injection of pentobarbitone sodium (Eutha 77R Coopers Tierarzneimittel GmbH) with immediate exsanguination by severance of the branchial or femoral vein and femoral artery. All animals were examined externally, and a full macroscopic examination of all tissues and organs in situ was performed.

Retina Preparation

Eyes were enucleated and rinsed in phosphate-buffered saline, and adhering fat and muscle were removed. For cryostatic sections, eyes were frozen at −70°C. For wholemounts, eyes were fixed in 4% buffered formaldehyde solution and prepared no later than 4 to 7 days postmortem. In some cases, wholemount preparations were performed with retinas fixed in half-strength Karnovsky's fixative. Before preparation, the eyes were rinsed in water for 0.5 to 1.0 hour to remove fixative, then the posterior eye chamber was opened by a circumferential incision posterior to the processus ciliaris removing cornea, iris, lens, ciliary body, and most of the vitreous body. The retina carefully was peeled away from the pigment epithelium and detached from the ora serrata. The retina was dissected into three sections, leaving the optic nerve head and macula intact, each section being mounted in Apathy's gum syrup mounting medium on a glass slide with a coverslip. The orientation of the wholemounted retina always was with the nerve fiber layer up. Examination of wholemounts using polarization, differential interference contrast, and bright field microscopy followed immediately after specimen preparation.

Cryostatic, 8- to 10-μm sections were prepared from unfixed frozen whole eyes or, in some cases, from paraformaldehyde/glutaraldehyde fixed portions of globes, then stained with aqueous Mayer's hematoxylin and mounted in crystal mount medium (Biomeda, Foster City, CA) at 50°C. Paraffin sections for histopathologic analysis were prepared and stained with hematoxylin–eosin according to standard procedures used for routine disease.

High-Performance Liquid Chromatography Analysis of Canthaxanthin and Other Carotenoids in Retinas

For chemical analysis of canthaxanthin (Bausch and Liechti, unpublished data), the left retina of each animal was isolated immediately postmortem and frozen at −70°C. Lyophilized retinas were extracted with 10% ethanol in n-hexane, containing 0.05% butyl-hydroxytoluene. After evaporation under nitrogen at 30°C, the residue was redissolved in n-hexane/dichloromethane (1:1, vol:vol) and submitted to HPLC. The HPLC conditions were as follows: column, 220 mm, 4.6 mm ø; stationary phase, spheri-5 silica, 5 μm (Brownlee Columns, Applied Biosystems, Santa Clara, CA), desactivated with N-ethyldiisopropylamine.

Detection was performed using a diode array detector (Hewlett Packard 1090; Hewlett Packard, Waldbronn, Germany) at a wavelength of 470 nm. Purities of the carotenoid peaks were established by spectra in the range of 350 to 600 nm. Typical retention times for all-trans canthaxanthin, 9-cis and 13-cis canthaxanthin, 4'hydroxy-echinenone, and isozeaxanthin were 17.7, 18.0, 19.8, and 21.8 minutes, respectively. The limit of detection for all-trans canthaxanthin was 250 pg. Recoveries from spiked samples were between 85% for isozeaxanthin and 4'hydroxy-echinenone and 98% for the canthaxanthin isomers. All-trans canthaxanthin and canthaxanthin isomer concentrations were expressed in nanogram/retina, canthaxanthin metabolites in percent of all-trans canthaxanthin peak values. Zeaxanthin and lutein were identified based on spectral data.

Canthaxanthin Plasma Analysis

Plasma samples were obtained from all animals preterminally. Canthaxanthin plasma analysis was performed according to standard procedures established at F. Hoffmann-La Roche (unpublished data). Briefly, thawed samples were extracted with water/ethanol

per n-hexane, and HPLC was performed using Spherisorb Alumina 5 μm with n-hexane/acetone (92:8) as eluent. Photometric detection limit was 20 μg/l canthaxanthin at 470 nm.

RESULTS

Clinical Retinal Examination

Clinical ophthalmoscopy and retinal biomicroscopy of both experimental and placebo animals showed no paramacular retinal crystals nor were there any treatment-related pathologic lesions.

Electroretinography

After 12 and 24 months, no parameter of the ERG showed any statistically significant, treatment-related change of amplitude or latency when compared to the placebo group nor to the historic background collective (scotopic, photopic, dark adaptation, and oscillatory potential amplitudes and latencies; $P \leq 0.05$).

Postmortem Investigations

Distribution and Microscopic Characteristics of Canthaxanthin-induced Inclusions in the Peripheral Retina. Microscopic examination results of retinal wholemounts of canthaxanthin-treated monkeys showed the presence of birefringent inclusions within a peripheral, circular zone of the retina (Fig. 1A), visualized as brightly shining, orange-yellow spots in polarized light. Highest densities were observed in the group with 16.2 mg canthaxanthin/kg/body weight per day. The incidence of these inclusions diminished from the ora serrata toward the posterior pole (Fig. 1C). The width of the zone containing inclusions was dose related, that is, from ~5 mm in the group with 5.4 mg/kg/body weight per day to 8 to 10 mm or larger in the group with 16.2 mg/kg/body weight per day (Fig. 1C). Retinas from placebo animals did not show any birefringent inclusions (Fig. 1B). At higher magnification, birefringent inclusions in retinal wholemounts appeared as glittering reddish, red, orange, or greenish-white entities in polarized light (Fig. 2A). They were located irregularly in the inner layers of the retina. In bright field, the same inclusions were reddish to orange brown and also very often (but not exclusively) arranged as islets close to blood vessels (Fig. 2B). Their morphology varied from rods to needles or microgranules of sizes between >1 and ~6 μm (Figs. 2C, 2D). Increasing proportions of larger particles predominantly were observed in animals of the 16.2 mg/kg/body weight per day and 48.6 mg/kg/body weight per day dose groups. Histologic examination results of frozen sections of peripheral retina showed birefringent inclusions in the inner retinal layers, for example, in the nerve fiber layer, ganglion cell layer, inner plexiform layer, inner nuclear layer, and to a lesser extent in the outer plexiform layer but not the outer nuclear layer, photoreceptors, nor the retinal pigment epithelium (RPE) (Fig. 2E). No crystalline deposits were observed within the choroid or the RPE (Fig. 2E). Isolated large, orange or red particles were seen frequently in the inner plexiform layer of animals receiving higher doses. Toward the center of the retina, round-to-oval inclusions of similar size and bright yellowish–orange-to-white color were associated frequently with isolated ganglion cells (Figs. 3A,

FIGURE 1. Distribution of canthaxanthin-induced inclusions in wholemounts of peripheral retina of (**A**) a female animal receiving 16.2 mg canthaxanthin/kg/body weight per day; carotenoid inclusions are visible as bright, shining spots; (**B**) a placebo-treated male animal; OS: ora serrata. (**C**) Retina wholemount from the same animal as in A. The photographs were taken from consecutive parts of the retina, orientated from the ora serrata (*left*) to the center (*right*), covering a distance of approximately 8 mm. Note the decreasing incidence of inclusions toward the center. Polarization, ×40.

FIGURE 2. Microscopic characteristics of canthaxanthin-induced inclusions. (**A**) Sector of wholemounted, peripheral retina from a male animal fed 16.2 mg canthaxanthin/kg/body weight per day, showing numerous birefringent inclusions with high light reflection in polarized light. Note the reddish, orange, or bright yellow color of the inclusions and the islet-like arrangements (*arrows*) close to a blood vessel. Polarization, ×150. (**B**) Identical sector as in A, bright field, showing the ganglion cell layer. Note the islet-like arrangement of reddish brown, microgranular particles (*arrows*) close to a blood vessel that correspond to those marked in A. Bright field, ×150. (**C**) Polymorphous, birefringent retinal inclusions in an animal fed 48.6 mg/kg/body weight per day with strongly light reflecting needles, microgranules, and clumps (*arrows*). Polarization, ×300. (**D**) Identical sector as in C showing the orange, yellowish color of the structures marked in C (*arrows*), and their irregular distribution throughout the ganglion cell layer–inner plexiform layer. Differential interference contrast, ×300. (**E**) Cryostatic section of the peripheral retina of a male monkey fed 5.4 mg canthaxanthin/kg/body weight per day. Birefringent inclusions are located in the ganglion cell layer, inner plexiform layer, and inner nuclear layer. Polarization, ×150.

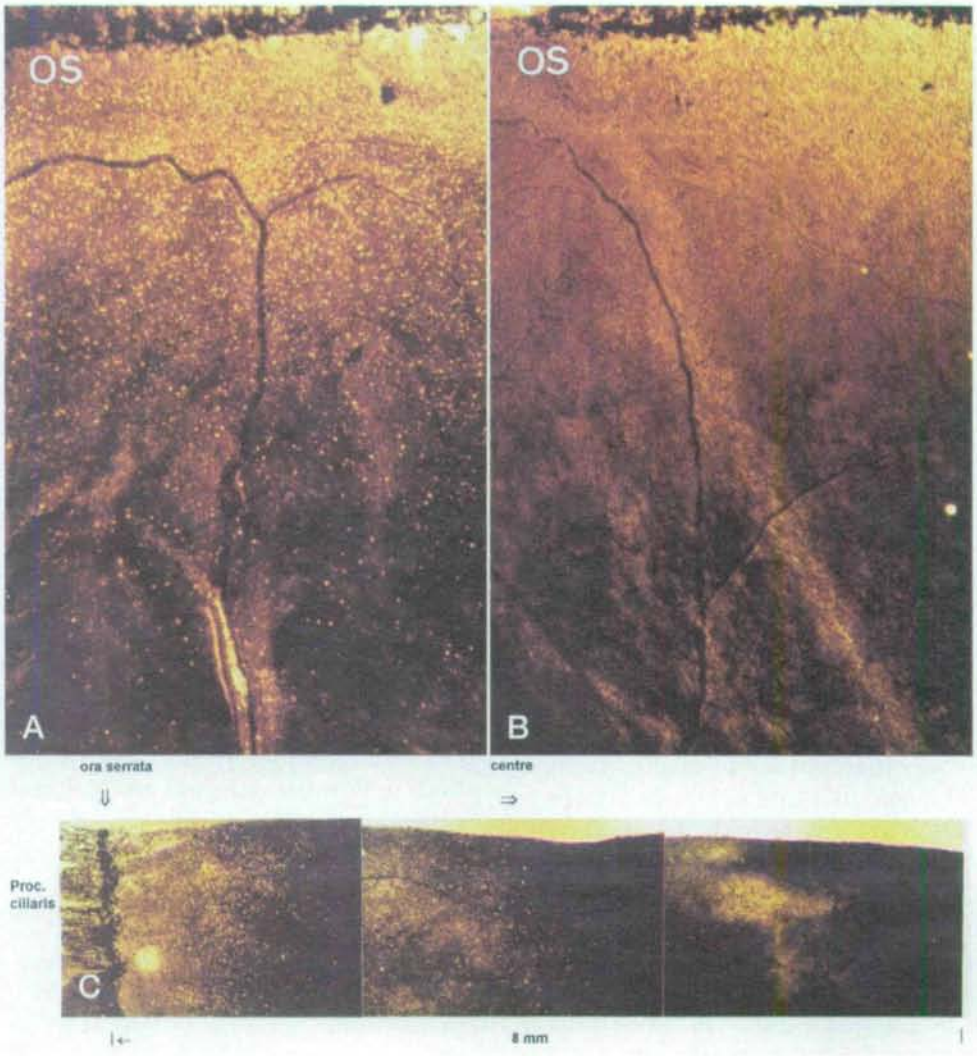

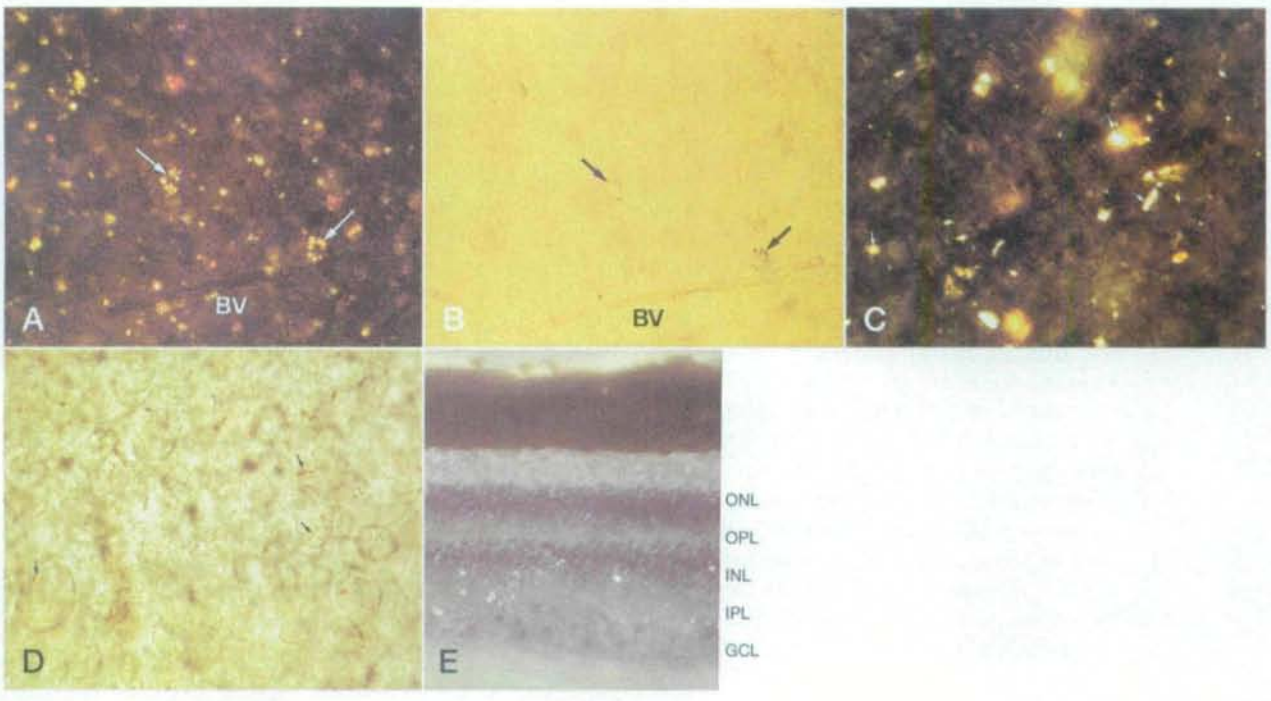

3B), possibly also with amacrine cells in the inner plexiform layer, adjacent to the inner nuclear layer (Fig. 3E). Localization of a crystal inside the perikaryon or occasionally inside the cellular process (Figs. 3C, 3D, 3F) was attributable only for this type of islet-like accumulations. The precise localization of all other birefringent inclusions was not possible with the techniques used.

Microscopic Characteristics of Macular Inclusions. In prepared retinas, the macular yellow spot, normally present in any primate retina, appeared macroscopically to be a more intense yellow color in all canthaxanthin-treated animals than those of placebo-treated animals, which relatively were pale. A clinically observable perimacular zone of crystals did not develop in any of the canthaxanthin-treated animals as seen typically in humans taking high dosages of canthaxanthin. However, three animals of the 5.4 mg/kg/body weight per day group, five animals of the 16.2 mg/kg/body weight per day group, and four animals of the 48.6 mg/kg/body weight per day group showed very small (<1 μm) rod-like inclusions in flat-mounted foveal–parafoveal areas. These particles appeared golden birefringent in polarized light (Figs. 4A, 4C) and yellow-to-orange in bright field (Fig. 4D). Just as with the peripheral birefringent inclusions, they also were located in the inner retinal layers but not in the photoreceptor layer. Because of the thickness of these whole-mounted tissues, a definite localization as to depth was not possible. When present, macular inclusions were observed in greatest number in those animals treated with 16.2 mg/kg/body weight per day. Placebo-treated animals showed no birefringency in the macula (Fig. 4B).

Retina Histopathologic Analysis

In paraffin sections that were prepared using organic solvents known to solubilize canthaxanthin, birefringent inclusions were not observed in any part of the retina. There also were no overt spaces in the inner layers of the peripheral retina, especially at the ganglion cells level, which would mark localization of an eluted foreign material. Dissociation within fiber layers or optically empty spaces (e.g., around cell nuclei) was seen in both control and treated animals and was assumed to be fixation artifacts. Proportions of the different retinal layers within corresponding radial sections were comparable in control or treated animals.

Canthaxanthin Plasma Concentrations

Preterminal canthaxanthin plasma levels in treated animals were dose related (Table 1) ($r = 0.756$), but increases were nonlinear. Highly variable levels of individual animals resulted in high standard deviations for the groups. Mean concentrations ranged from 2018 ± 839 μg/l in the 5.4 mg/kg/body weight per day dose group to 4400 ± 1682 in the 48.6 mg/kg/body weight per day dose group. Canthaxanthin concentration in plasma correlated with retina concentrations ($r = 0.784$).

Canthaxanthin Retina Concentrations

All-trans canthaxanthin, its 9-cis/13-cis isomers, and canthaxanthin-derived compounds 4′-OH-echinenone and isozeaxanthin only were present in retinas of treated animals (summarized in Table 1). A typical HPLC chromatogram of an animal treated with 48.6 mg/kg/body weight per day is shown in Figure 5. All-trans canthaxanthin

FIGURE 3. Localization of canthaxanthin-induced inclusions in relation to retina cell structures. (**A**) Wholemount of peripheral retina of an animal on 16.2 mg canthaxanthin/kg/body weight per day. Birefringent bright yellowish microgranules are arranged as nest-like islets. Polarization, ×750. (**B**) Identical sector as in A, showing the location of the inclusions in the cytoplasm of two ganglion cells in the peripheral retina. Differential interference contrast, ×750. (**C**) Strongly light reflecting microgranules in the peripheral retina of a male animal on 16.2 mg canthaxanthin/kg/body weight per day, showing a nest-like arrangement, with single particles aligning like a chain (*arrows*) toward the blood vessel on the right side of the picture. The diffuse, whitish polarizing structures present in these sector are artifacts due to fixation. Polarization, ×750. (**D**) Identical sector as in C, differential interference contrast. Microgranules inside the perikaryon of a bipolar cell. To the right, the axon of the cell, which is protruding toward the blood vessel, contains chain-like aligned, orange-colored particles (*arrows*). Differential interference contrast, ×750. (**E**) Cryostatic section of the peripheral retina of a male monkey (same animal as in Fig. 2) on 48.6 mg canthaxanthin/kg/body weight per day showing a large bright orange birefringent inclusion (*arrowhead*) in the inner plexiform layer adjacent to the inner nuclear layer, single, more whitish shining, presumably amacrine cell-associated (*small arrow*), and GCL-associated inclusions. Polarization, ×750. (**F**) Similar cryostatic section as in E (i.e., from the same animal as in Figs. 2 and 5E), showing accumulation of birefringent inclusions associated with a ganglion cell and its cellular process arising from the inner nuclear layer. Polarization, ×750.

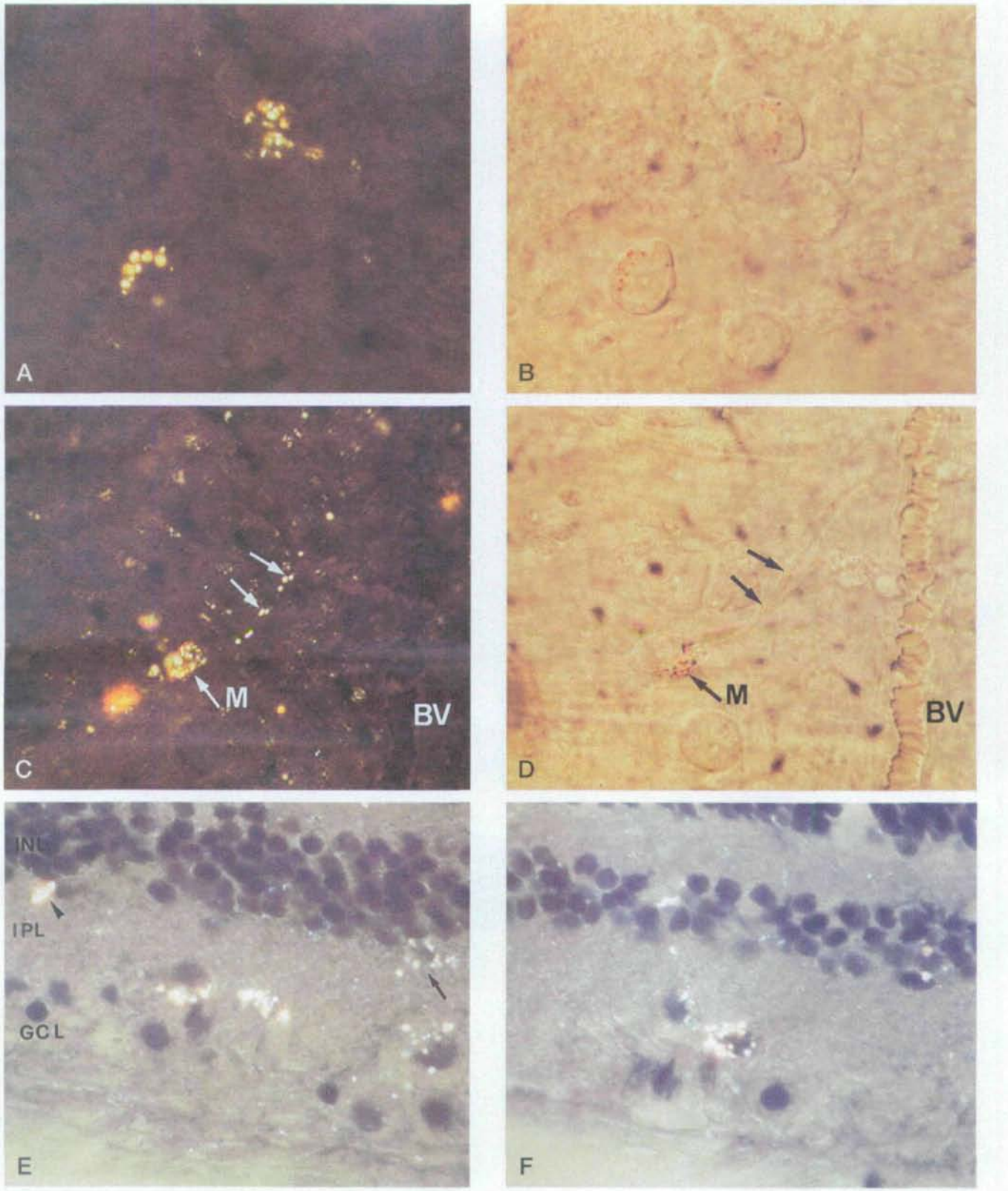

concentrations varied considerably among individuals on the same dose. Whereas there was an increase of all–trans canthaxanthin concentrations (mean ± standard deviation) from 130.25 ± 100.37 ng/retina in the group with 5.4 mg/kg/body weight per day to 257.18 ± 137.65 ng/retina in the group with 16.2 mg/kg/body weight per day, there was a decrease to 173.86 ± 132.44 ng/retina in the group with 48.6 mg/kg/body weight per day. Canthaxanthin concentration in the retina correlated well with plasma concentrations (see above). In all treated animals, concentrations of 9-cis/13-cis isomers were approximately 15% of those of all–transcanthaxanthin con-

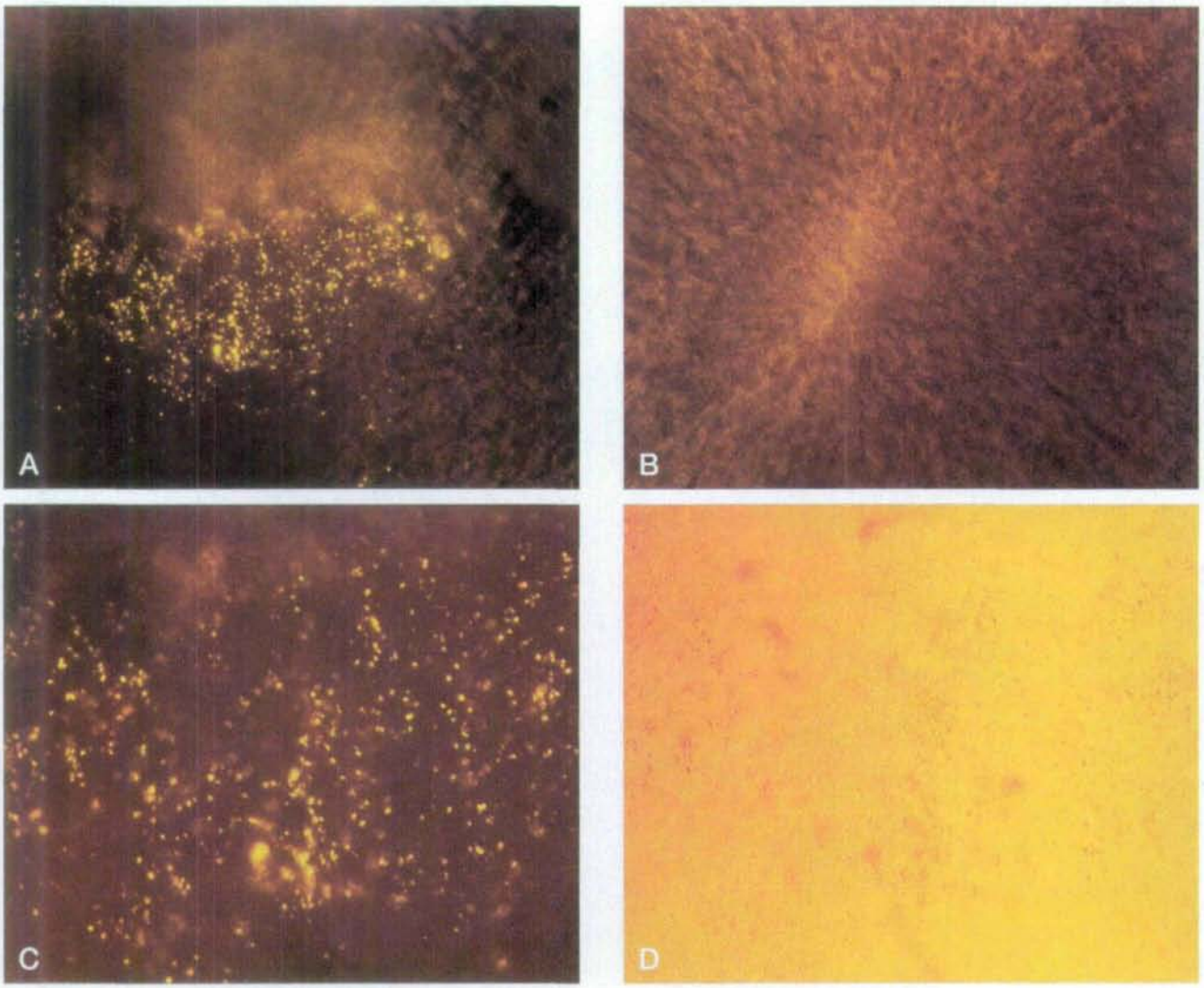

FIGURE 4. Macular canthaxanthin-induced inclusions in retinal wholemounts. (**A**) Fovea–foveal slope of a female animal fed 16.2 mg canthaxanthin/kg/body weight per day with tiny yellow, golden birefringent structures. Polarization, ×300. (**B**) Fovea–foveal slope of a placebo-treated, female animal without polarizing structures. Polarization, ×300. (**C**) Higher magnification of the golden yellowish structures from A. Polarization, ×750. (**D**) Identical sector as in C showing the orange color and rod–droplet-like morphology of the birefringent structures in bright field. Polarization, ×750.

centrations. 4′-OH-echinenone and isozeaxanthin concentrations increased dose dependently. In all treated groups, relative levels of 4′-OH-echinenone were approximately 36.0%, and of isozeaxanthin, 5.5% of retinal all-trans canthaxanthin peak values. The macular pigments lutein and zeaxanthin were detected in retinas of all animals. Their relative amounts per retina as represented by the peak areas varied considerably and were not dependent on canthaxanthin treatment. There were no gender-related differences in the concentrations of all analyzed carotenoids between male and female monkeys.

DISCUSSION

Microscopic and chemical investigations of the eyes of cynomolgus monkeys treated with canthaxanthin for 2.5 years showed that the formation of crystal-like inclusions occurs in the retina in association with high dosages of the compound. All 24 animals treated with doses from 5.4 to 48.6 mg canthaxanthin/kg/body weight per day had formed birefringent inclusions in the retinal periphery, and in 12 of them also in the paramacular area. In contrast to the phenomenon observed in humans, where canthaxanthin crystals were seen clinically as perimacular, "glittering" spots, in monkeys, these crystals were not detectable within the central retinal area by conventional in vivo ophthalmoscopy nor retinal biomicroscopy.

Localization and Characteristics of Retinal Inclusions

Canthaxanthin inclusions were distributed in the retinas in their highest densities near the ora serrata with dimin-

TABLE 1. Canthaxanthin in Retina and Plasma

Dose		Retina				Plasma
		Canthaxanthin Isomers [ng/retina]		Canthaxanthin-Derived Compounds [% of all-trans canthaxanthin]		Canthaxanthin Plasma Concentration [μg/L]
mg/kg per day	n	All-trans canthaxanthin	9-cis/13.cis canthaxanthin	4'-OH-echinenone	Isozeaxanthin	All-trans canthaxanthin
0	8	0.7 ± 0.4	<DL*	<DL*	<DL*	<DL†
5.4	8	130.3 ± 100.4	20.01 ± 16.0	37.9 ± 4.3	5.8 ± 0.9	2018 ± 839
16.2	8	257.2 ± 137.6	38.01 ± 18.7	36.7 ± 6.8	5.7 ± 2.1	3089 ± 1062
48.6	8	173.9 ± 132.4	25.61 ± 22.3	35.9 ± 6.9	4.9 ± 1.5	4400 ± 1682

* DL = detection limit in high-pressure liquid chromatography retina analysis: 250 pg.
† DL = detection limit in high-pressure liquid chromatography plasma analysis: 20 μg canthaxanthin/l plasma.

ishing density toward the center. Although this finding generally is similar to that of Daicker et al,[4] who studied the one known human postmortem retina, it differs regarding the variability of crystal density and size as a function of retinal location. Daicker et al[4] observed a tinted red, 2.5- to 3.0-mm wide crystal-containing ring near the ora serrata, the crystals ranging between 4 and 25 μm with the larger inclusions occurring paracentrally. In contrast, the monkeys in this study showed polarizing inclusions having a maximum length of only 10 μm at their farthest peripheral location but decreasing in size to a much smaller 2 μm in the macular area. This >10 times difference in inclusion size explains their clinical invisibility in monkeys compared with that of humans. At 25 μm, the human crystals subtend a visual angle of just more than 3 minutes of arc on ophthalmoscopy, which is just larger than the expected minimum angle of resolution of the examiner's vision (1 minute of arc). In contrast, the approximately 2-μm central inclusions of the monkeys, at 0.2 minute of arc, fall well below the examiner's visual clinical resolution ability. The occurrence of birefringent particles was not dependent on specific cell structures in the far periphery. A location inside the processes of Müller cells, which wrap all neuronal cells, as postulated by Daicker et al,[4] certainly is possible but will require further detailed analysis (e.g., by immunolabeling of glial proteins). Nevertheless, in this monkey study, at a distance of approximately 5 to 8 mm from the ora serrata, birefrin-

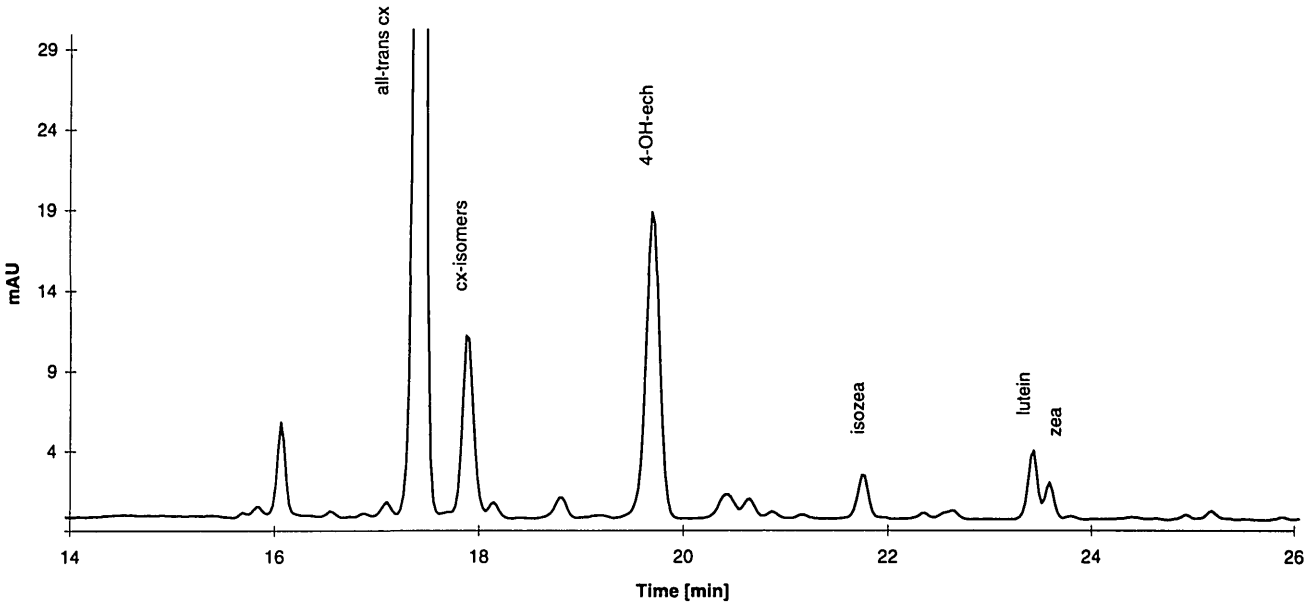

FIGURE 5. High-performance liquid chromatography of a retinal extract from a male animal treated with 48.6 mg canthaxanthin/kg/body weight per day. All-trans cx: all-trans canthaxanthin; retention time (RT), 17.4 minutes; cx-isomers: 9-cis/13-cis canthaxanthin isomers, RT, 17.8 minutes; 4'-OH-ech: all-trans 4'-OH-echinenone, RT, 19.6 minutes; isozea: all-trans isozeaxanthin, RT, 21.7 minutes; lutein: all-trans lutein, RT, 23.4 minutes; zea: all-trans zeaxanthin, RT, 23.5 minutes. (Diode array detection, signal wavelength 470.4 nm, reference wavelength 590.24 nm.)

gent particles seemed to be present preferentially within ganglion cells.

The reason for the preferential distribution in the periphery and for the location in the inner retinal layers is not known. The absence of choroidal deposition could imply that canthaxanthin enters the retina through the retinal vascular system arising from the central retinal artery and not from the choriocapillaris. This idea also is supported by the finding that ganglion cells, containing canthaxanthin inclusions, also were often observed in the neighborhood or directly adjacent to blood vessels or capillaries. The retinal vasculature of primates consists of several capillary network planes and Snodderly and Weinhaus[18] mention that the thin retinal periphery contains a single, superficial plane at the junction of the retinal and ganglion cell layers. This was the location at which peripheral inclusions in the monkey were observed most frequently.

If canthaxanthin were to enter the retina through the retinal vascular system, this would imply that its capillary endothelium is permeable for canthaxanthin, or that a specific transport mechanism exists. Similarly, in considering the possibility of supplying canthaxanthin to the retina through the choriocapillaris, the tight junctions of the RPE form an intact blood–retinal barrier, necessitating carrier proteins for effective retinal transport.[19] The RPE has a key role in maintaining the retina through supplying it with nutrients, delivering 70% to 80% of the oxygen, and in resorbing degradation products from the tips of the photoreceptor outer segments.[20] If canthaxanthin had entered the retina through the choriocapillaris system and the RPE, it might accumulate preferentially in the outer retinal layers and photoreceptor segments, which are rich in membranes and lipids, especially phospholipids.[21] However, we have never observed canthaxanthin inclusions in the photoreceptor layer or in the RPE. Nevertheless, entry through the choriocapillaris still is a possibility if an effective intraretinal transport mechanism, such as the Müller cell, exists that would move canthaxanthin inwardly within the retina. In the monkeys, the area around the macula and the optical disc was free of crystals, whereas in the fovea and particularly in the parafoveal slope, birefringent inclusions with different morphologic appearance ("droplet rod-like") and dichroic properties like those of the periphery were detected. Because they had uniform oval shapes, these inclusions may have arisen from carotenoid containing lipid droplets. Similar to those in the periphery, they were localized in the inner retinal layers and not in the photoreceptor layer of cones. In the same central area of the retina are located the normally occurring macular yellow pigments zeaxanthin and lutein. These carotenoids reside within the receptor axon layer (Henle fiber) and inner plexiform layer.[22,23] The intensely yellow-colored maculas of treated monkeys and the localization of zeaxanthin and lutein together with canthaxanthin in these retinae also suggest that these more-droplet to rod-like inclusions may be composed of a mixture of zeaxanthin–lutein with canthaxanthin or other canthaxanthin-derived compounds or both (e.g., 4'hydroxyechinenone or isozeaxanthin).

Electroretinography

The presence of canthaxanthin deposits in the cytoplasm of retinal ganglion cells and other inner layer locations did not interfere with retinal functions. The ERGs taken after 1 and 2 years of treatment were within normal clinical ranges and did not differ significantly in any measured component when compared with both the placebo and the historic control groups. In contrast to the slight, reversible b-wave changes noted in humans after canthaxanthin ingestion,[3] no abnormalities in the b-wave amplitude or latency were measured. Because the b-wave is attributable to the response of the glial Müller cell, it has been implicated in the theoretical mechanism of canthaxanthin-induced retinopathy in humans.[3] Of particular importance in this study was the lack of any significant change in ERG oscillatory potentials, even though there was clear histologic evidence of ganglion cell inclusions, thus indicating no functional effect of these ganglion cell inclusions.

Canthaxanthin Analysis in Retinas

Chemical analysis proved that canthaxanthin was present in the retinas of all treated animals in an all-trans to cis ratio similar to that of the beadlet formulation used for dosing. Although retinal concentrations of canthaxanthin achieved during the study showed increasing levels between the lowest dose group (5.4 mg/kg/body weight per day) and the middle dose group (16.2 mg/kg/body weight per day), this dose-response effect showed a trailing off at the highest dose (48.6 mg/kg/body weight per day). Also, retinal canthaxanthin concentrations correlated well generally with the incidence of inclusions in the retinas, being the highest in the 16.2 mg/kg/body weight per day group.

The relatively high variability of canthaxanthin retinal concentration among animals on the same dose indicates that substantial individual metabolic differences may exist. This is not surprising because similar high levels of individual variation are described for macular yellow pigment densities in humans and nonhuman primates, including significant differences in homozygous twins,[24] thus suggesting environmental effects also may be in play.

Because 4-hydroxyechinenone and isozeaxanthin were present at approximately 40% of all-trans canthaxanthin concentrations, it may be concluded that the birefringent inclusions observed, especially in the pe-

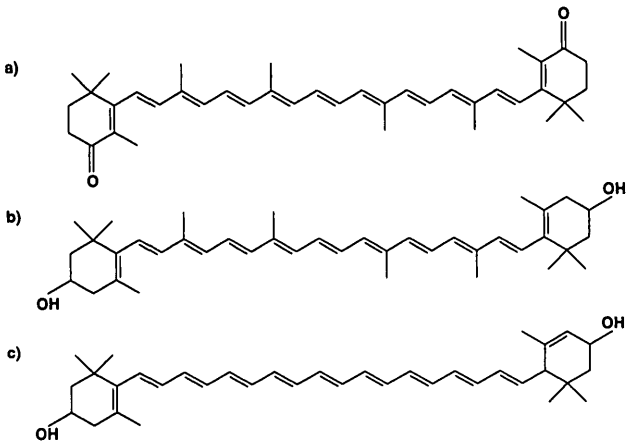

FIGURE 6. Chemical structures of all-trans canthaxanthin (**A**) and the macular yellow pigments zeaxanthin (**B**) and lutein (**C**).

ripheral retina, probably were composed of canthaxanthin isomers (trans and cis) and canthaxanthin-derived compounds. 4-OH-echinenone and isozeaxanthin have been suggested to be metabolites of the reductive canthaxanthin pathway in chicken and other nonmammalian species.[25] They also have been detected by Daicker et al[4] in human eye tissues after high canthaxanthin intake. Zeaxanthin and lutein concentrations in the central retina varied considerably but were not influenced by increasing amounts of canthaxanthin. Zeaxanthin and lutein are both polar, diet-derived xanthophylls (Fig. 6) and currently represent the main carotenoids identified physiologically in primate retinas and maculas.[11,26] Because polarity seems to be associated with retina entry and because the 4-oxo-group of canthaxanthin confers polarity to the molecule, it can be speculated that canthaxanthin uses the similar transport mechanisms as zeaxanthin and lutein. In humans[27] and primates (W. Cohn, unpublished data), the main fraction of canthaxanthin is transported in the plasma through low density lipoproteins. It is well established that molecules carried by low density lipoprotein particles enter cells by the specific mechanism of low density lipoprotein receptor-mediated endocytosis. Thus, one proposed hypothesis for canthaxanthin uptake in retina cells can be based on this mechanism, which includes binding using coated pits, invagination of the cell membrane, and formation of intracellular-coated vesicles. Consequently, canthaxanthin would be expected to accumulate in the cytoplasm inside membrane vesicles. The morphology of the uniform, round-to-oval inclusions inside the perikaryon of ganglion cells, which resembled granulated vesicles in light microscopy, substantiates such a hypothesis. Furthermore, although birefringent and dichroic, this type of particle did not appear as that of typical crystals. It seems likely that they were associated with lipoproteins as suggested by Daicker et al.[4]

Canthaxanthin Concentration in Plasma

Preterminal all-trans canthaxanthin concentrations in plasma of treated monkeys were dose dependent. Plasma concentrations achieved on the lowest dose of 5.4 mg/kg/body weight per day for 2.5 years (2018 μg/l) gave rise to retinal inclusions in all animals of this group. Canthaxanthin plasma levels of patients with retinal crystals have not been reported. In a kinetic study of canthaxanthin resorption in humans, a single dose of 150 mg (approximately 2.5 mg/kg/body weight) led to plasma concentrations of 4.3 μmol/l (equivalent to 2429 μg/l) after 7 to 8 hours.[27] This is similar to our results of preterminal levels of the monkeys. In contrast, plasma levels of ferrets fed 50 mg canthaxanthin/kg/body weight per day for 1 month were 100-fold lower.[28] In addition, retinal crystal formation has not been observed in this species, even after 2 years' treatment (unpublished data). In contrast, the chicken, which as a species normally incorporates carotenoids within the retinal structures, achieves similarly high canthaxanthin plasma levels (2000 to 9000 μg/l) when fed up to 80 mg canthaxanthin/kg/body weight per day for 6 weeks (Goralczyk et al, unpublished data).

In summary, because histologically visible retinal inclusions developed in all treated monkeys, it can be concluded that the threshold level for crystallization is lower than 5.4 mg/kg/body weight per day. The intake of humans in whom retinal inclusions developed is not known precisely. Recent statistical evaluations[5] of 411 crystal cases with known canthaxanthin dosage information show a highly significant dose-response relation. Intakes < 30 mg canthaxanthin daily (i.e., approximately 0.5 mg/kg/body weight per day) did not lead to crystal formation. But these levels were for clinically observable crystals. To establish a no-effect level in monkeys, further evaluations with lower dosages currently are underway.

Our results show that the cynomolgus monkey is an adequate animal model to study the crystallization of canthaxanthin in the retina. High, chronic intake led to the inclusion of birefringent retinal carotenoid crystals with a typical distribution pattern. Adverse effects on visual functions were not detectable. Many questions concerning the transport, entry, and subcellular localization of canthaxanthin in the retina remain open and require further investigations.

Key Words

canthaxanthin, carotenoid, electroretinography, monkey, retina

Acknowledgments

The authors thank Hams Liechti (Basel) for expert technical assistance; Dr. Ute Korte (Münster) for routine ophthalmoscopy; and Drs. Willi Cohn (Basel), Wolfgang Köpcke (Münster), Mamfred Lützow, Wolfgang Schalch, Katharina

Schiedt (Basel), and Eberhard Zrenner (Tübingen) for valuable discussions and expert advice.

References

1. Mathews-Roth MM. Carotenoids quench evolution of excited species in epidermis exposed to UV-B (290–320 nm) light. *Photochem Photobiol.* 1986;43:91–93.
2. Cortin P, Corriveau LA, Rousseau AP, Tardif Y, Malenfant M, Boudreault G. Maculopathie en paillettes d'or. *Can J Ophthalmol.* 1982;17:103–106.
3. Arden GB, Barker FM. Canthaxanthin and the eye: A critical ocular toxicological assessment. *J Toxicol—Cut & Ocular Toxicol.* 1991;10:115–155.
4. Daicker B, Schiedt K, Adnet JJ, Bermond P. Canthaxanthin retinopathy: An investigation by light and electron microscopy and physicochemical analysis. *Graefes Arch Clin Exp Ophthalmol.* 1987;235:189–197.
5. Köpcke W, Barker FM, Schalch W. Canthaxanthin deposition in the Retina: A biostatistical evaluation of 411 patients. *J Toxicol—Cut & Ocular Toxicol.* 1994;14:89–104.
6. Chang TS, Aylward GW, Clarkson JG, Gass JDM. Asymmetric canthaxanthin retinopathy. *Am J Ophthalmol.* 1995;119:801–802.
7. Scallon LJ, Burke JM, Mieler WF, et al. Canthaxanthin-induced retinal pigment epithelium changes in the cat. *Curr Eye Res.* 1988;7:687–693.
8. Weber U, Kern W, Novotny GEK, et al. Experimental carotenoid retinopathy I: Functional and morphological alterations of the rabbit retina after 11 month of dietary carotenoid application. *Graefes Arch Clin Exp Ophthalmol.* 1987;225:198–205.
9. Barker FM, Fox JG, Teller B, Blanco MC. The ferret ERG in high dosage canthaxanthin administration. ECORA Meeting, October 1993, Bonn, Germany.
10. Harnois C, Kubawara T, Boudreault G. Canthaxanthin retinopathy in monkeys: Clinical and histopathological studies. ARVO Abstracts. *Invest Ophthalmol Vis Sci.* 1990;31:139.
11. Bone RA, Landrum JT, Tarsis SL. Preliminary identification of the human macular pigment. *Vision Res.* 1985;25:1531–1535.
12. Handelman GJ, Dratz EA, Reay CC, van Kuijk JGM. Carotenoids in the human macula and whole retina. *Invest Ophthalmol Vis Sci.* 1988;29:850–855.
13. Handelman GJ, Snodderly DM, Krinsky NI, Russel MD, Adler AJ. Biological control of primate macular pigment. *Invest Ophthalmol Vis Sci.* 1991;32:257–267.
14. Will OH, Scovel CA. Photoprotective functions of carotenoids. In: Krinsky NI, Mathews-Roth MM, Taylor RF, eds. *Carotenoids, Chemistry and Biology.* New York: Plenum Press; 1990:229–236.
15. Schalch W. Carotenoids in the retina—A review of their possible role in preventing or limiting damage caused by light and oxygen. In: Emrit T, Chance b, eds. *Free Radicals and Aging.* Basel: Birkhäuser Verlag; 1992:280–298.
16. Bee WH, Korte R, Vogel F. Electroretinography in the non-human primate as standardized method in toxicology. In: Weisse I, Hockwin O, Tripathi RC, eds. Ocular Toxicology: Proceedings of the 4th Congress of the International Society of Ocular Toxicology, Annecy, France, October 9–13, 1994. New York: Plenum Press; 1995:53–61.
17. Marmor MF, Arden GB, Nilsson SEG, Zrenner E. Standard for clinical electroretinography. *Arch Ophthalmol.* 1989;107:816–819.
18. Snodderly DM, Weinhaus RS. Retinal vasculature of the fovea of the squirrel monkey, Saimiri sciureus: Three dimensional architecture, visual screening, and relationships to to the neuronal layers. *J Comp Neurol.* 1990;297:145–163.
19. Bok D. Retinal photoreceptor-pigment epithelium interactions. ARVO Abstracts. *Invest Ophthalmol Vis Sci.* 1985;26:1659.
20. Handelman GJ, Dratz EA. The role of antioxidants in the retina and retinal pigment epithelium and the nature of prooxidant-induced damage. *Adv Free Radiol Biol Med.* 1986;2:1–89.
21. Fliesler JF, Anderson RE. Chemistry and metabolism of lipids in the vertebrate retina. *Prog Lipid Res.* 1983;22:79–131.
22. Snodderly DM, Brown PK, Delori FC, Auran JD. The macular pigment I: Absorbance spectra, localization, and discrimination from other yellow pigments in primate retina. *Invest Ophthalmol Vis Sci.* 1984;25:660–673.
23. Bone RA, Landrum JT. Macular pigment in the Henle'fibre membranes: A model for Haidinger's brushes. *Vision Res.* 1984;24:103–108.
24. Hammond BR, Fuld K, Curran-Celentano J. Macular pigment density in monozygotic twins. *Invest Ophthalmol Vis Sci.* 1995;36:2531–2541.
25. Schiedt K. New aspects of carotenoid metabolism in animals. In: Krinsky NI, Mathews-Roth MM, Taylor RF, eds. *Carotenoids, Chemistry and Biology.* New York: Plenum Press; 1990:247–268.
26. Handelman GJ, Dratz EA, Reay CC, van Kuijk FJ. Carotenoids in the human macula and whole retina. *Invest Ophthalmol Vis Sci.* 1988;29:850–855.
27. Von Reinersdorff D. *Biokinetische Untersuchungen zur Resorption von Canthaxanthin.* Giessen, Germany: Justus-Liebig-Universität Giessen; 1990. Dissertation. In German.
28. Tang G, Dolnikowsky GG, Blanco MC, Fox JG, Russel RM. Serum carotenoids and retinoids in ferrets fed canthaxanthin. *J Nutr Biochem.* 1993;4:58–63.